PURPOSE-LED PUBLISHING™

NOTE • **OPEN ACCESS**

Bioactive Uio-66 coating on polydopamine-modified titanium implants

To cite this article: Aslı Ece Gümüşkaya *et al* 2026 *Biomed. Mater.* **21** 041001

View the article online for updates and enhancements.

You may also like

- Synergistically enhanced aspirin loading and pH-triggered controlled release via a ZIF-L/ZIF-8 hierarchical coating on titanium
Shanchun Zhang, Xiangyu Cheng, Jingtong Wu et al.
- The design of novel nanostructures on titanium by solution chemistry for an improved osteoblast response
V V Divya Rani, K Manzoor, Deepthy Menon et al.
- Surface Modification of Titanium with Functional and Bio-Molecules by Electrodeposition to Add Biofunctions
Takao Hanawa and Yusuke Tsutsumi

This content was downloaded from IP address 80.251.45.167 on 10/08/2026 at 22:18

Biomedical Materials

Check for updates

NOTE

Bioactive Uio-66 coating on polydopamine-modified titanium implants

Aslı Ece Gümüşkaya[1], Berna Topuz[1], Sezin Galioglu[2] and Ayşe Karakeçili[1,*]

[1] Department of Chemical Engineering, Faculty of Engineering, Ankara University, 06100 Tandoğan, Ankara, Türkiye
[2] UNAM-National Nanotechnology Research Center Bilkent University, 06800 Ankara, Türkiye
[*] Author to whom any correspondence should be addressed.

E-mail: akarakecili@eng.ankara.edu.tr

Keywords: metal-organic framework, Zr-MOF, bioactive coating, polydopamine

Supplementary material for this article is available online

OPEN ACCESS

RECEIVED
18 February 2026

REVISED
14 July 2026

ACCEPTED FOR PUBLICATION
17 July 2026

PUBLISHED
30 July 2026

Original content from this work may be used under the terms of the Creative Commons Attribution 4.0 licence.

Any further distribution of this work must maintain attribution to the author(s) and the title of the work, journal citation and DOI.

Abstract

Engineering the surface of titanium (Ti) with bioactive coatings is an effective approach to address biofunctional limitations of Ti implants, including low bioactivity and poor tissue integration. Here, Ti substrates were functionalized with the UiO-66 metal–organic framework (MOF) via a polydopamine-assisted coating strategy to enhance cell–Ti implant interactions. The colloidal coating results in the formation of well-controlled surface with moderate hydrophilicity (water contact angle ∼70°) and a reduced local surface roughness value (Ra ∼23 nm) relative to *in situ* growth (Ra ∼76 nm). The optimized coating strategy developed in this study reveals that MOF nanocrystal loading, surface roughness, hydrophilicity and wettability critically determine the biointerface behavior and overall coating performance. The resulting hybrid morphology further promotes MC3T3-E1 cell viability on the implant surface while maintaining structural stability.

1. Introduction

Titanium and titanium alloys with desirable features as biocompatible materials with suitable mechanical properties have been extensively applied in repairing bone defects and substituting dysfunctional hard tissue especially in orthopedic implants [1, 2]. Despite the excellent biocompatibility and strong corrosion resistance, titanium implants are bioinert, usually resulting in poor osteogenesis due to inadequate integration with surrounding bone tissue. To address this challenge, developing a bioactive coating to alter the surface properties of titanium is regarded as a cost-effective and efficient approach [2–4]. A zirconium-based metal–organic framework (MOF), UiO-66, is distinguished by its low cytotoxicity, good biocompatibility, high chemical and thermal stability, and robust Zr–O coordination bonds. Recently, our group has demonstrated that UiO-66 serves as a reservoir for Zr ions, providing prolonged osteogenic stimulation and osteoblastic differentiation, while its robust face-centered cubic framework ensures structural integrity even under physiological conditions [5, 6]. Furthermore, coating of Ti implants with MOFs as effective surface modification agents in bone regeneration has attracted growing attention to achieve bioactive surfaces. Considering cytocompatibility, MOF structures incorporating osteogenic ions have been coated onto Ti implants to improve osteogenic activity [3, 7–9] Meanwhile, most of these modifications include complex chemical cues. Furthermore, owing to the limited presence of reactive functional groups on Ti surface, deposition of MOF structures onto bare Ti surfaces is disadvantageous in terms of stability. The mussel-inspired bioadhesive polydopamine (PDA) formed by the self-polymerization of monomers and can form *in situ* on metal surfaces via the covalent cohesion while avoiding relatively complicated chemical modifications [3, 10, 11]. Zhou *et al* have reported the synthesis of UiO-66 and UiO-66-NH_2 membranes onto aluminum surfaces through a polydopamine assisted method. They have utilized UiO-66-NH_2 as firm anchor sites for covalently grafting with superhydrophobic molecules, enabling robust, high performance anti-corrosion as-prepared coatings [12]. Herein, UiO-66 MOF nanocrystals were coated/immobilized onto Ti substrates using the PDA assisted process. The coating process was carried out using two different strategies: *in situ* coating or colloidal coating. To the

© 2026 The Author(s). Published by IOP Publishing Ltd

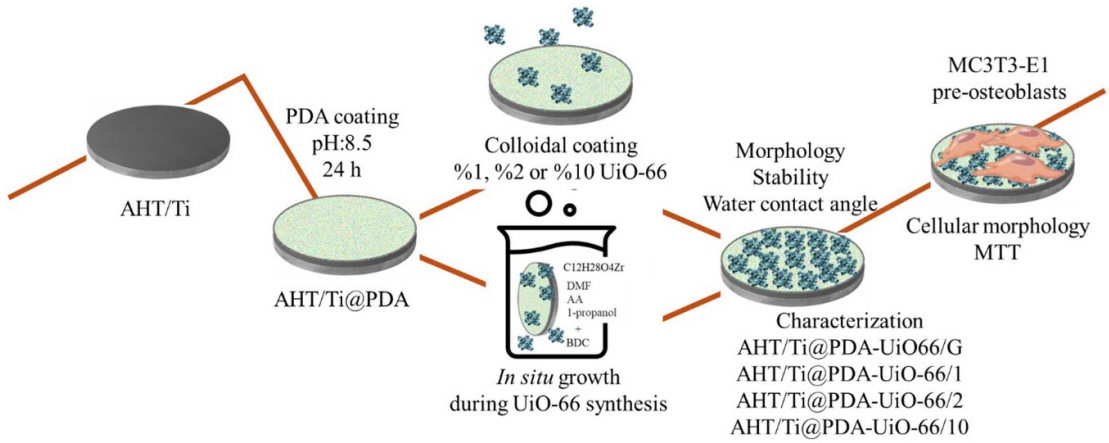


Figure 1. Schematic representation of UiO-66 coating process and characterization.

best of our knowledge, PDA assisted UiO-66 immobilized/coated Ti implants have been investigated for the first time in the literature in terms of evaluating the coating strategies, substrate surface properties, surface coverage, morphology, hydrophilicity and viability of MC3T3-E1 pre-osteoblast cells (figure 1).

2. Materials and methods

2.1. Materials

Titanium plates (Ti, commercially available, Grade 1, 12 mm in diameter and 1 mm in thickness) were supplied by a local producer in Turkey. Acetone (C_3H_6O) used for cleaning the plates was obtained from Merck, and ethanol (C_2H_5OH) was purchased from ISOLAB. Sodium hydroxide (NaOH) used for surface modification of the titanium plates, dopamine hydrochloride and Tris-HCl used for surface coating were obtained from Sigma-Aldrich (Germany). Zirconium (IV) propoxide solution (70% w/w in 1-propanol), 1-propanol, N,N-Dimethylformamide (DMF, anhydrous 99.8%), acetic acid (AA) and terephthalic acid (BDC, 98%)) were purchased from Sigma-Aldrich (Germany). For cell culture studies, α-MEM (containing L-glutamine), trypsin-EDTA and Dulbecco's Phosphate Buffered Saline (DPBS) were purchased from Biowest (France). Fetal bovine serum (FBS), penicillin-streptomycin (pen/strep), and Thiazolyl Blue Tetrazolium Bromide (MTT, ⩾98%) were obtained from Sigma-Aldrich (Germany). Glutaraldehyde (25% w/w in H_2O) was purchased from Merck (Germany).

2.2. Synthesis of UiO-66 nanocrystals and modification of AHT/Ti@PDA with UiO-66

UiO-66 nanocrystals were synthesized using a previously reported solvothermal method [5, 13]. Briefly, 355 µl zirconium (IV) propoxide were mixed in 35 ml DMF, 20 ml AA, 322.5 µl 1-propanol and the mixture was kept at 130 °C for 2 h. After cooling down to room temperature, 375 mg BDC was added to the solution as a linker and stirred at 250 rpm for 24 h at 35 °C. Subsequently, the product was collected by centrifugation at 21 130 RCF for 20 min and washed three times in DMF followed by another washing step in absolute ethanol. Finally, UiO-66 nanocrystals were dried at 40 °C overnight and kept in a desiccator for further use.

Ti substrates were ultrasonically washed with acetone, ethanol and deionized water for 15 min and dried in an oven at 37 °C. Clean and dry Ti plates were immersed in 5 M NaOH solution for 24 h at 60 °C. Afterwards, the samples were rinsed three times in deionized water for 15 min each and dried at 37 °C for 24 h. Subsequently, the substrates were heated to 600 °C at a rate of 5 °C min^{-1} in an electrical furnace for 1 h. The surface treated substrates were referred as alkali-heat treated/Ti (AHT/Ti). For PDA coating, AHT/Ti substrates were immersed in a dopamine hydrochloride solution (2 mg ml^{-1} in Tris buffer, pH = 8.5) for 24 h. Afterwards, the samples were rinsed in DI water and dried at 37 °C. These substrates were referred as: AHT/Ti@PDA [10].

The surface modification via UiO-66 was performed using two different approaches; *(i) in situ coating*, which involves the growth of UiO-66 on the AHT/Ti@PDA substrate during the synthesis of UiO-66, or *(ii) colloidal coating*, which involves deposition/immobilization of pre-synthesized UiO-66 onto the AHT/Ti@PDA substrate. In the first approach of *in situ* coating, UiO-66 synthesis was realized in the presence of AHT/Ti@PDA substrates. The substrates were vertically immersed in the pre-mixture of DMF, AA, 1-propanol, and zirconium (IV) propoxide at room temperature. Then, BDC

was added to the solution, and the reaction mixture was stirred at 250 rpm for 24 h at 35 °C to allow the growth of UiO-66 nanocrystals directly on substrates surfaces (AHT/Ti@PDA-UiO66-G). In the second approach of, *colloidal coating process*, the pre-synthesized UiO-66 were immobilized/deposited onto AHT/Ti@PDA substrates in a colloidal suspension medium containing different amounts of UiO-66 for 2 h at room temperature. Subsequently, the surfaces were ultrasonically cleaned using DI water to remove un-attached UiO-66 and dried at 40 °C for 24 h (AHT/Ti@PDA-UiO66/1, AHT/Ti@PDA-UiO66/2 and AHT/Ti@PDA-UiO66/10 for 1%, 2% and 10% (w/v) UiO-66 concentration, respectively) [14].

2.3. Characterization and cell viability evaluation

The substrate morphology was analyzed with scanning electron microscope (SEM, QUANTA 400 F Field Emission) and energy-dispersive x-ray spectroscopy (EDAX). Prior to imaging, the SEM samples were coated with a thin layer of Au–Pd alloy via sputtering. The surface wettability and hydrophilicity of the samples were determined by water contact angle (WCA) measurements. The measurements were performed at three different points on each sample, using the static drop method with 1 µl DI water droplets at room temperature, employing a contact angle measurement device (WCA, KRUSS Drop Shape Analyzer). Surface morphology and roughness of the samples were characterized using atomic force microscope (AFM, PSIA) operating in non-contact mode. All measurements were performed at a scan rate of 1 Hz. The scan size was set to 5 × 5 μm^2. Surface roughness values were extracted from the AFM images using standard image analysis software. To evaluate the stability of the nanocrystals immobilized/coated on the surfaces, the samples were incubated in α-MEM at 37 °C for 7 d and analyzed by SEM.

In vitro cell culture studies were performed using MC3T3-E1 pre-osteoblasts (RIKEN Cell Bank, Japan) to assess the cell viability [13]. Cells were seeded on each sample (1×10^5 cell) and allowed to proliferate in osteogenic medium (α-MEM supplemented with 10% (*v/v*) FBS, 10 mM β-glycerol phosphate, and 50 µg ml^{-1} ascorbic acid). MTT assay was performed at 4 and 7 d of culture. The detailed procedure is given in Supplementary File. Cellular morphology was observed on the 7th day of the culture. The sample plates were removed from the culture medium, gently washed in DPBS and placed in 2.5% (w/v) glutaraldehyde solution for 30 min at room temperature. Subsequently, the samples were washed in DPBS and DI and freeze-dried at −80 °C for 24 h using a lyophilizator (Christ, Germany). The samples were coated with Au–Pd prior to SEM analysis [15]. All experiments were performed with at least three independent samples. Difference between p values <0.05 was considered as statistically significant.

3. Results and discussion

UiO-66 nanocrystals were synthesized and characterized as described, previously [5, 6]. The uniform octahedral morphology was successfully synthesized, as confirmed by SEM imaging (figure 2), consistent with our previous findings [5, 6]. The diffraction pattern of synthesized UiO-66 nanocrystals was consistent with the simulated pattern (figure S1) indicating the crystallization of phase-pure UiO-66. FTIR-ATR spectrum shows the characteristic peaks related to UiO-66 (figure S1).

The morphological characterization of Ti and modified Ti substrates is presented in figure 2. PDA coating on metallic implants is a versatile strategy to increase biocompatibility, enabling the immobilization of bioactive agents via its mussel-inspired adhesive motifs to enhance osteogenesis and vascularization [10]. Herein, the main purpose of the PDA coating was to enhance the interfacial binding between the UiO-66 and AHT/Ti surfaces, thereby leading to stable coatings. In our preliminary experiments we have observed that application of UiO-66 on AHT/Ti surface resulted in an unstable coating where nanocrystals detached from the surface when in contact with aqueous environment after ∼1 h (data not shown).

As shown in figure 2, UiO-66 nanocrystals grown directly on the AHT/Ti@PDA implant surface during the synthesis reaction formed a highly dense and continuous coating in which multilayers of UiO-66 nanocrystals were clearly observed on AHT/Ti@PDA-UiO66/G. The EDAX spectrum reveals the prominent peaks corresponding to carbon (C) and oxygen (O) originating from the BDC linker and zirconium (Zr) originating from the metal node in UiO-66 (figure S2). The enhanced stability for coating/immobilization is possibly due to the Π-cation interactions between the catechol groups in PDA and Zr ions in UiO-66. In contrast, colloidal coating of AHT/Ti@PDA substrates obtained via deposition of UiO-66 colloidal suspensions highly depended on the UiO-66 concentration in the suspension. The lowest coating coverage was observed for AHT/Ti@PDA surfaces immersed in a 1% UiO-66 suspension. The EDAX displayed the presence of Zr at approximately <0.1%. Therefore, AHT/Ti@PDA-UiO66/1 samples were excluded from subsequent *in vitro* cell culture studies as these samples were considered insufficient to elicit a cellular response in terms of

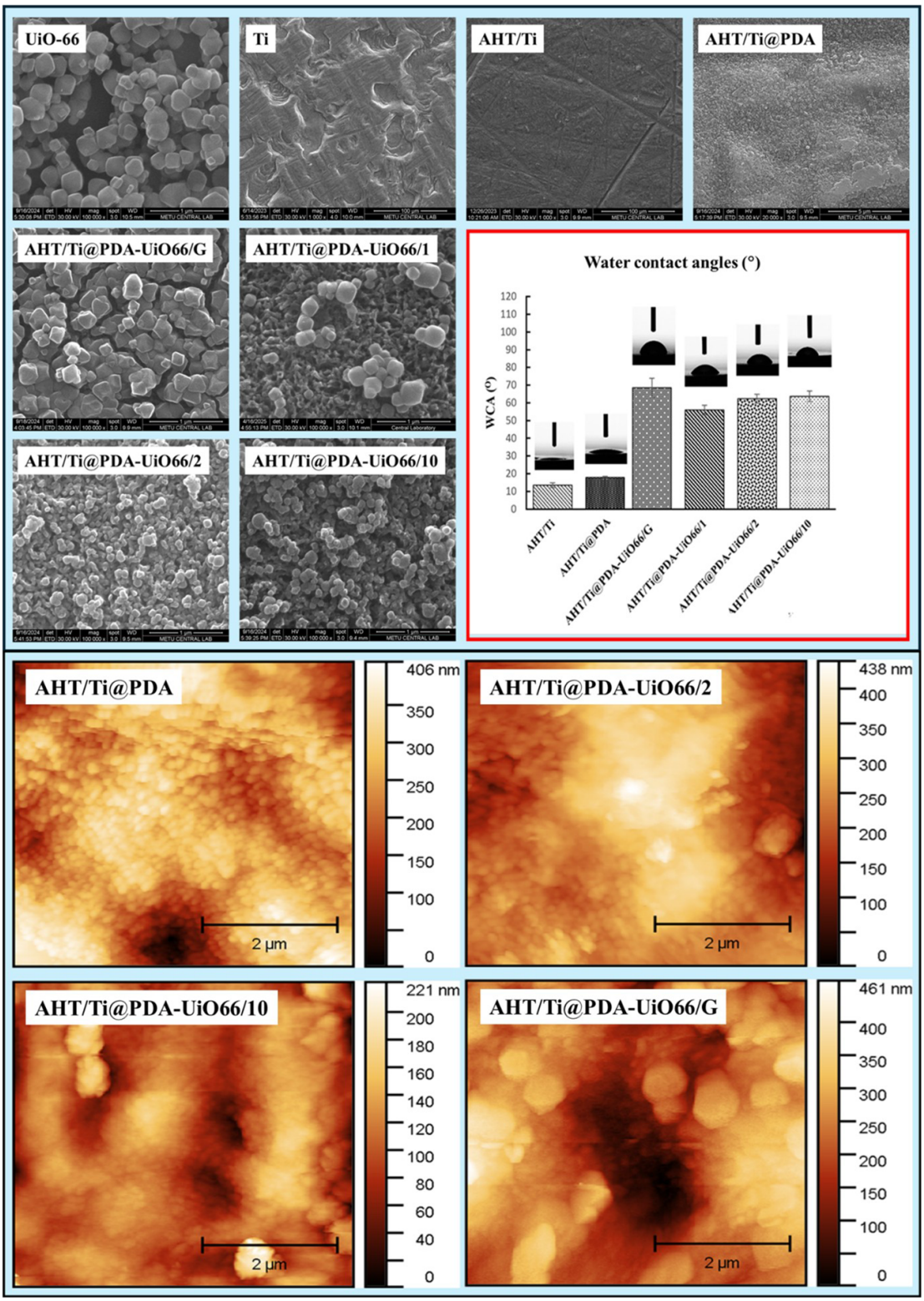


Figure 2. SEM images of UiO-66 nanocrystals along with Ti, modified Ti and UiO-66 coated Ti surfaces. WCA measurements demonstrate the wettability of the substrates. AFM images illustrate the roughness.

UiO-66 amount. Increasing the suspension concentration to 2% and 10% (w/v) resulted in a marked increase in surface coverage. The WCA values obtained for AHT/Ti, AHT/Ti@PDA, AHT/Ti@PDA-UiO66/G, AHT/Ti@PDA-UiO66/1, AHT/Ti@PDA-UiO66/2 and AHT/Ti@PDA-UiO66/10 samples are $13.5 \pm 1.2°$, $17.7 \pm 0.7°$, $68.5 \pm 5.4°$, $56.1 \pm 2.6°$, $62.2 \pm 2.5°$ and $63.7 \pm 3.1°$, respectively (figure 2). AHT/Ti and AHT/Ti@PDA exhibited high surface hydrophilicity (WCA $< 20°$). After UiO-66 coating the WCA notably increased. The highest WCA was obtained for AHT/Ti@PDA-UiO66/G. Direct

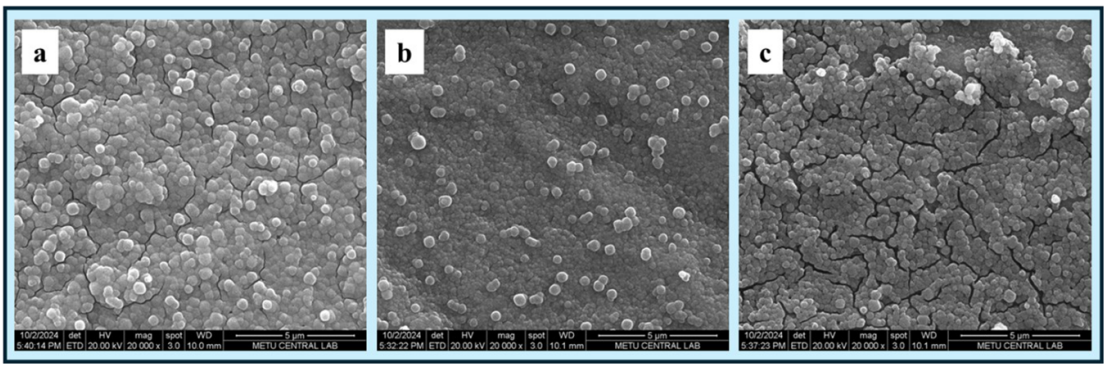


Figure 3. Stability evaluation in α-MEM after 7 d for AHT/Ti@PDA-UiO66/G (a), AHT/Ti@PDA-UiO66/2 (b) and AHT/Ti@PDA-UiO66/10 (c). It is evident that the UiO-66 morphology was preserved, and surface coverage was stable.

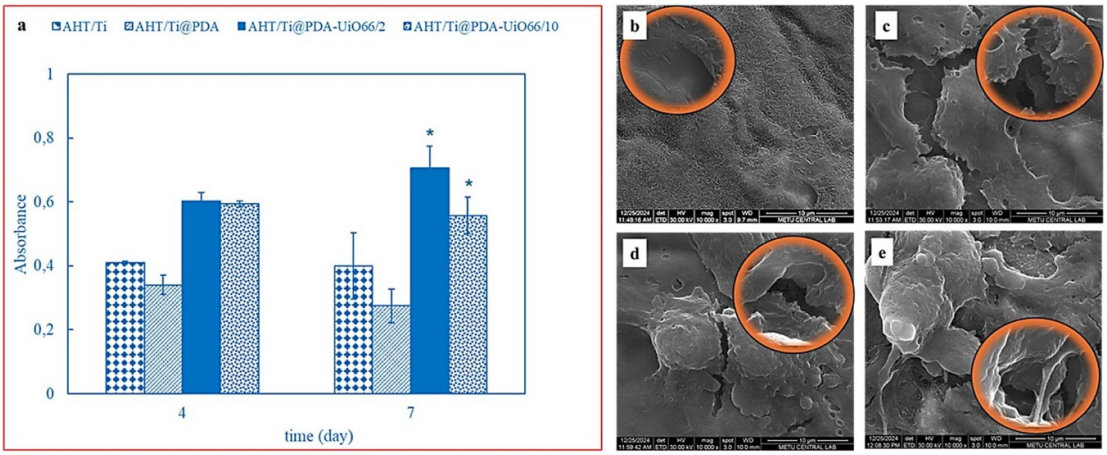


Figure 4. MTT assay (a), cellular morphology on AHT/Ti (x10 000) (b), AHT/Ti@PDA (c), AHT/Ti@PDA-UiO66/2 (d) and AHT/Ti@PDA-UiO66/10 (e). $^{*}p < 0.001$ when AHT/Ti@PDA is control. Orange circled inserts show (x50 000).

crystallization of UiO-66 via *in situ* growth forms a dense and interlocked crystal layer that restricts water penetration into the underlying surface. In the colloidal coating approach, the WCA of substrates increased with increasing UiO-66 concentration, likely due to enhanced surface coverage. The randomly distributed nanocrystal layer and interparticle voids may facilitate the infiltration of water droplet and consequently lead to lower contact angle. It is also noteworthy to mention that the increased surface roughness of densely UiO-66–coated surfaces may have contributed to the higher contact angle values. AFM analysis further showed that the AHT/Ti-PDA underlying surface was progressively covered, leading to a decrease in the local average Ra value of 69 ± 25 nm to 23 ± 5 nm as the UiO-66 concentration increased from 2% to 10% (w/v) (figure 2). However, the excessive growth during the *in situ* coating process resulted in non-uniform accumulation of UiO-66 nanocrystals, yielding the highest surface roughness (76 ± 24 nm).

The stability of UiO-66 coating in terms of persistent surface coverage and UiO-66 nanocrystal morphology has been evaluated by SEM analysis. Figure 3 depicts the AHT/Ti@PDA-UiO66/G, AHT/Ti@PDA-UiO66/2 and AHT/Ti@PDA-UiO66/10 substrates after being treated in α-MEM for 7 d.

The viability and proliferation of MC3T3-E1 cells are depicted in figure 4. AHT/Ti and AHT/Ti@PDA surfaces supported the cell proliferation as reported, previously (figure 4(a)) [7]. Meanwhile, in the present study, the primary objective of employing a PDA coating was to establish an intermediate layer to mediate UiO-66 immobilization/coating in a biocompatible manner [16]. As confirmed by our results, coating of UiO-66 has promoted MC3T3-E1 cell viability on both AHT/Ti@PDA-UiO66/2 and AHT/Ti@PDA-UiO66/10 substrates. However, MTT assay demonstrated that the cell viability was considerably reduced on AHT/Ti@PDA-UiO66/G substrates (low absorbance values of 0.04 ± 0.005 on day 4) related to the extensive surface accumula-

tion achieved via *in situ* growth strategy. We have observed similar results in our previous study, in which the cell viability decreased in the presence of increased amount of UiO-66 in 3D-printed scaffolds [6]. SEM images show that the cells on AHT/Ti surfaces were observed in round structure, unclear morphology (figure 4(b)). Meanwhile, cells cultured on AHT/Ti@PDA surfaces displayed lamellar morphology (figure 4(c)). It was evident that UiO-66 immobilization/coating increased the cellular interactions, as depicted in figures 4(d) and (e). The filapodial extensions were distinctively pronounced on AHT/Ti@PDA-UiO66/10 surfaces (figure 4(e), inset, figure S3). Overall, WCA and the surface roughness results point out moderate hydrophilicity (WCA $\sim 70^{\circ}$) and a smoother surface that promotes cellular interactions after UiO-66 coating.

4. Conclusion

We reported stable coating of UiO-66 onto AHT/Ti@PDA surfaces where PDA served as an intermediate layer. The *in situ* growth strategy, which does not allow control over the amount of UiO-66 immobilized on the surface, failed to support MC3T3-E1 pre-osteoblast attachment, adhesion, and proliferation, likely due to cytotoxic effects associated with extensive surface accumulation. In contrast, the colloidal coating method enabled concentration-dependent control of coating, and no cytotoxic effects were observed even at the highest tested concentration of 10% (w/v). Consequently, the UiO-66 MOF structure, known for the osteogenic stimulatory role of its Zr ions, was successfully used to modify pristine Ti implant surfaces by PDA assisted strategy, pointing out a promising potential for our future *in vivo* studies and prospects for osseointegration of titanium implants.

Acknowledgment

This research was funded by Ankara University-FYL-2024-3406.

Data availability statement

The data cannot be made publicly available upon publication because they are not available in a format that is sufficiently accessible or reusable by other researchers. The data that support the findings of this study are available upon reasonable request from the authors.

Supplementary Material available at: https://doi.org/10.1088/1748-605X/ae8c9d/data1.

ORCID iDs

Berna Topuz 0000-0002-6980-3296
Sezin Galioglu 0000-0001-5369-9546
Ayşe Karakeçili 0000-0002-8857-4927

References

[1] Xia Z, Sun X, Mu C, Wang K, Ma W, Yang W and Xu K 2025 An enhanced osseointegration of titanium implants by H_2S sustained-release coating via promoting osteogenesis and inhibiting osteoclastogenesis *Adv. Healthcare Mater.* **14** 2404940
[2] Li J, Zheng Y, Yu Z, Kankala R K, Lin Q, Shi J, Chen C, Luo K, Chen A and Zhong Q 2024 Surface-modified titanium and titanium-based alloys for improved osteogenesis: a critical review *Heliyon* **10** e23779
[3] Si Y, Liu H, Yu H, Jiang X and Sun D 2022 MOF-derived CuO@ZnO modified titanium implant for synergistic antibacterial ability, osteogenesis and angiogenesis *Colloids Surf. B* **219** 112840
[4] Malheiros S S, Borges M H R, Rangel E C, Fortulan C, da Cruz N C, Barao V A R and Nagay B E 2025 Zinc-doped antibacterial coating as a single approach to unlock multifunctional and highly resistant titanium implant surfaces *ACS Appl. Mater. Interfaces* **17** 18022–45
[5] Karakeçili A, Topuz B, Ersoy F Ş and Şahin T 2022 UiO-66 metal-organic framework as a double actor in chitosan scaffolds: antibiotic carrier and osteogenesis promoter *Biomater. Adv.* **136** 212757
[6] Gunyakti Mujtaba A, Altunay B B, Pinarbasi B, Topuz B, Yilgor P and Karakeçili A 2025 Zr-based metal-organic framework nanocrystals improve the osteoinductivity and osteogenicity of alginate/methyl cellulose bioink *Int. J. Biol. Macromol.* **313** 144255
[7] Wu J *et al* 2022 Surface modification of the Ti surface with nanoscale bio-MOF-1 for improving biocompatibility and osteointegration *in vitro* and in vivo *J. Mater. Chem. B* **10** 8535–48
[8] Jakubowski M, Domke A, Voelkel A and Sandomierski M 2023 Biomedical applications of titanium alloys modified with MOFs—current knowledge and further development directions *Crystals* **13** 257
[9] Sandomierski M, Jakubowski M, Ratajczak M and Voelkel A 2022 Zeolitic imidazolate framework 8 (ZIF-8) modified titanium alloy for controlled release of drugs for osteoporosis *Sci. Rep.* **12** 9103
[10] Lv F, Gan N, Huang J, Hu F, Cao Y, Zhou Y, Dong Y, Zhang L and Jiang S 2017 A polydopamine-based metal-organic framework coating of the type PDA-MIL-53(Fe) for ultrasound-assisted solid-phase microextraction of polychlorinated biphenyls prior to their determination by GC–MS *Microchim. Acta* **184** 2561–8
[11] Liu X, Yue T, Qi K, Xia B Y, Chen Z, Qiu Y and Guo X 2020 Probe into metal-organic framework membranes fabricated via versatile polydopamine-assisted approach onto metal surfaces as anticorrosion coatings *Corros. Sci.* **177** 108949
[12] Zhou J, Wang Z, Liu R, Qi K, Qiu Y and Guo X 2024 UiO-66 and UiO-66-NH_2 membranes-based superhydrophobic coatings for enhanced corrosion protection *Prog. Org. Coat.* **194** 108575

[13] DeStefano M R, Islamoglu T, Garibay S J, Hupp J T and Farha O K 2017 Room-temperature synthesis of UiO-66 and thermal modulation of densities of defect sites *Chem. Mater.* **29** 1357–61
[14] Yan B, Tan J, Zhang H, Liu L, Chen L, Qiao Y and Liu X 2022 Constructing fluorine-doped Zr-MOF films on titanium for antibacteria, anti-inflammation, and osteogenesis *Biomater. Adv.* **134** 112699
[15] Toprak Ö, Topuz B, Monsef Y A, Oto Ç, Orhan K and Karakeçili A 2021 BMP-6 carrying metal-organic framework embedded in bioresorbable electrospun fibers for enhanced bone regeneration *Mater. Sci. Eng. C* **120** 111738
[16] Jia L, Han F, Wang H, Zhu C, Guo Q, Li J, Zhao Z, Zhang Q, Zhu X and Li B 2019 Polydopamine-assisted surface modification for orthopaedic implants *Orthop. Transl.* **17** 82–95